NASA/TM-2003-212033

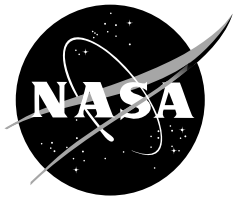

A Fuzzy Technique for Performing Lateral-Axis Formation Flight Navigation Using Wingtip Vortices

Curtis E. Hanson
NASA Dryden Flight Research Center
Edwards, California

September 2003

The NASA STI Program Office…in Profile

Since its founding, NASA has been dedicated to the advancement of aeronautics and space science. The NASA Scientific and Technical Information (STI) Program Office plays a key part in helping NASA maintain this important role.

The NASA STI Program Office is operated by Langley Research Center, the lead center for NASA's scientific and technical information. The NASA STI Program Office provides access to the NASA STI Database, the largest collection of aeronautical and space science STI in the world. The Program Office is also NASA's institutional mechanism for disseminating the results of its research and development activities. These results are published by NASA in the NASA STI Report Series, which includes the following report types:

- TECHNICAL PUBLICATION. Reports of completed research or a major significant phase of research that present the results of NASA programs and include extensive data or theoretical analysis. Includes compilations of significant scientific and technical data and information deemed to be of continuing reference value. NASA's counterpart of peer-reviewed formal professional papers but has less stringent limitations on manuscript length and extent of graphic presentations.

- TECHNICAL MEMORANDUM. Scientific and technical findings that are preliminary or of specialized interest, e.g., quick release reports, working papers, and bibliographies that contain minimal annotation. Does not contain extensive analysis.

- CONTRACTOR REPORT. Scientific and technical findings by NASA-sponsored contractors and grantees.

- CONFERENCE PUBLICATION. Collected papers from scientific and technical conferences, symposia, seminars, or other meetings sponsored or cosponsored by NASA.

- SPECIAL PUBLICATION. Scientific, technical, or historical information from NASA programs, projects, and mission, often concerned with subjects having substantial public interest.

- TECHNICAL TRANSLATION. English-language translations of foreign scientific and technical material pertinent to NASA's mission.

Specialized services that complement the STI Program Office's diverse offerings include creating custom thesauri, building customized databases, organizing and publishing research results…even providing videos.

For more information about the NASA STI Program Office, see the following:

- Access the NASA STI Program Home Page at ***http://www.sti.nasa.gov***

- E-mail your question via the Internet to help@sti.nasa.gov

- Fax your question to the NASA Access Help Desk at (301) 621-0134

- Telephone the NASA Access Help Desk at (301) 621-0390

- Write to:
  NASA Access Help Desk
  NASA Center for AeroSpace Information
  7121 Standard Drive
  Hanover, MD 21076-1320

NASA/TM-2003-212033

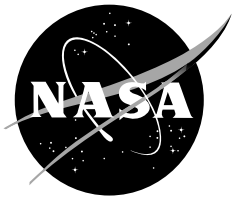

A Fuzzy Technique for Performing Lateral-Axis Formation Flight Navigation Using Wingtip Vortices

Curtis E. Hanson
NASA Dryden Flight Research Center
Edwards, California

National Aeronautics and
Space Administration

Dryden Flight Research Center
Edwards, California 93523-0273

September 2003

NOTICE

Use of trade names or names of manufacturers in this document does not constitute an official endorsement of such products or manufacturers, either expressed or implied, by the National Aeronautics and Space Administration.

Available from the following:

NASA Center for AeroSpace Information (CASI)
7121 Standard Drive
Hanover, MD 21076-1320
(301) 621-0390

National Technical Information Service (NTIS)
5285 Port Royal Road
Springfield, VA 22161-2171
(703) 487-4650

ABSTRACT

Close formation flight involving aerodynamic coupling through wingtip vortices shows significant promise to improve the efficiency of cooperative aircraft operations. Impediments to the application of this technology include intership communication required to establish precise relative positioning. This report proposes a method for estimating the lateral relative position between two aircraft in close formation flight through real-time estimates of the aerodynamic effects imparted by the leading airplane on the trailing airplane. A fuzzy algorithm is developed to map combinations of vortex-induced drag and roll effects to relative lateral spacing. The algorithm is refined using self-tuning techniques to provide lateral relative position estimates accurate to 14 in., well within the requirement to maintain significant levels of drag reduction. The fuzzy navigation algorithm is integrated with a leader-follower formation flight autopilot in a two-ship F/A-18 simulation with no intership communication modeled. It is shown that in the absence of measurements from the leading airplane the algorithm provides sufficient estimation of lateral formation spacing for the autopilot to maintain stable formation flight within the vortex. Formation autopilot trim commands are used to estimate vortex effects for the algorithm. The fuzzy algorithm is shown to operate satisfactorily with anticipated levels of input uncertainties.

NOMENCLATURE

Acronyms

AFF	Autonomous Formation Flight
GPS	global positioning system

Symbols

a	fuzzy input membership function breakpoint
A	fuzzy input set
b	fuzzy output membership function breakpoint
B	fuzzy output set
C	coefficient
G	transfer function
i	longitudinal unit vector
in.	inches
IL	output membership function inboard large
IM	output membership function inboard medium
IS	output membership function inboard small
IV	output membership function inboard very small
IX	output membership function inboard extra large

j	lateral unit vector
J	cost function
k	vertical unit vector
K	autopilot
K	number of fuzzy inference rules
m	number of fuzzy input sets
NJ	input membership function negative jumbo
NL	input membership function negative large
NM	input membership function negative medium
NS	input membership function negative small
NT	input membership function negative tiny
NV	input membership function negative very small
NX	input membership function negative extra large
OL	output membership function outboard large
OM	output membership function outboard medium
OS	output membership function outboard small
OV	output membership function outboard very small
OX	output membership function outboard extra large
P	number of training data points
PL	input membership function positive large
PM	input membership function positive medium
PS	input membership function positive small
PV	input membership function positive very small
PX	input membership function positive extra large
TL	output membership function trailing large
TM	output membership function trailing medium
TS	output membership function trailing small
WA	output membership function wingtips aligned
x	state vector
y	lateral relative position
ZZ	input membership function zero
α	degree of membership in a fuzzy input set
β	degree of membership in a fuzzy output set

δ	command
Δ	increment
ε	estimation error
η	tuning speed parameter
σ	dither ratio magnitude
ϕ	roll angle
ψ	heading angle

Subscripts

a	roll stick
cmd	command
D	drag
e	error
f	formation
F	formation
filt	filtered
H	heading
i	fuzzy input variable index
k	fuzzy output set index
l	rolling moment
L	leading airplane
p	training data index
r	rudder
t	throttle
T	trailing airplane

Superscripts

f	fuzzy
j	fuzzy input set identifier
n	number of fuzzy input variables

Notation

^	estimate
$\rightarrow$	unit vector
•	time derivative
–	centroid, state vector

INTRODUCTION

The use of wingtip vortex effects for navigation is a by-product of the well-documented concept of reduced drag and improved range through close formation flight.[1–3] The presence of the vortex causes large disturbances to the trailing airplane, particularly in the roll axis, and a great deal of pilot workload is required to trim the airplane.[4] To reduce demands on the pilot, significant research has been done in the development of automatic guidance and control laws for close formation flight.[5–8] These controllers typically assume that timely and accurate measurements are exchanged between the aircraft. Some of the hurdles to close formation flight in an operational environment are the cost and logistics required to provide a communication link between two aircraft that may be of different types and operated by different organizations.

The method of trajectory tracking can be used to perform close formation flight without intership communication,[9] but only if both aircraft measure their absolute trajectory locations in an identical manner. The current state-of-the-art for this type of navigation is the global positioning system (GPS). However, the elimination of intership communication prevents the coordination of selected satellites between GPS receivers on both aircraft, which can lead to large trajectory separations[10] and eliminate any measurable drag reduction.

Another approach to formation flight in the absence of additional communications equipment or sensors is peak-seeking control.[1,11] These algorithms typically rely upon the introduction of a dither signal to the commanded flight path of the aircraft for parameter identification purposes. The dither signal may cause ride quality issues in addition to reduced efficiency resulting from excessive throttling as aerodynamic forces constantly change.

This report proposes a method for estimating the lateral relative position between two aircraft in close formation flight by using real-time estimates of the aerodynamic effects imparted by the wingtip vortex of the leading airplane on the trailing airplane. A fuzzy logic algorithm is generated from the relationship between lateral separation of a formation of two F/A-18 aircraft (McDonnell Douglas Corporation, now The Boeing Company, St. Louis, Missouri; and Northrop Corporation, now Northrop Grumman, Newbury Park, California) and vortex-induced rolling moment and drag forces. Inputs to the algorithm are vortex effects estimated from the commanded outputs of the formation controller. The algorithm is tuned using F/A-18 aircraft vortex models and is then integrated with a leader-follower formation control system and implemented into a six degree-of-freedom simulation. The fuzzy logic algorithm provides sufficient estimation of the lateral formation spacing to allow the autopilot to maintain stable and accurate formation flight within the vortex without intership communication or predefined trajectories. An assumption is made that the leading airplane does not intentionally maneuver but rather attempts to maintain a constant heading in the face of atmospheric disturbances. This assumption is not overly

restrictive as the most likely applications of formation flight drag reduction are cruise operations. Unlike typical peak-seeking methods, the fuzzy algorithm does not adversely affect the flight path of the airplane in any way. Although the fuzzy algorithm is applied to leader-follower formation control, this approach could also be used to improve trajectory spacing problems related to uncorrelated GPS receivers in a trajectory tracking application.

Assuming that nose-to-tail separation is maintained by the trailing airplane through occasional pilot throttle inputs, a close formation flight autopilot requires navigation information in both the lateral and vertical dimensions.[12] This report, however, restricts itself to a single dimension to provide a detailed and succinct discussion. The axis chosen is the lateral axis, or horizontal axis normal to the flight path. Additional vortex effects that are modeled but not used in the estimation algorithm, such as side force and yawing moment, may hold promise in extending this research to a two-dimensional navigation solution.

FORMATION FLIGHT AND VORTEX EFFECTS

Consider a system of two similar aircraft flying in a leader-follower formation, as shown in figure 1. The leading airplane flies to a constant commanded heading, altitude, and velocity while the trailing airplane maintains a constant commanded three-dimensional offset from the leading airplane. An orthogonal coordinate system with unit vectors $\left[\vec{i}_f, \vec{j}_f, \vec{k}_f\right]$ is used to describe the relative positions between the aircraft, where $\vec{i}_f$ and $\vec{j}_f$ lie within a plane parallel to the surface of the earth and $\vec{i}_f$ is aligned with the velocity vector of the trailing airplane. The lateral relative position y between the aircraft is defined as the $\vec{j}_f$ component of the distance between the centers of gravity of the two aircraft.

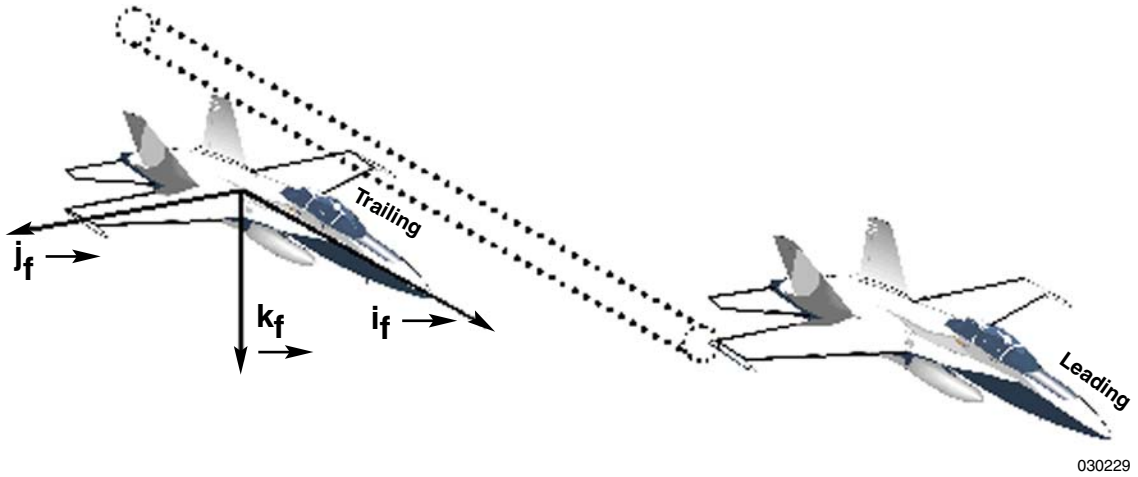

Figure 1. Leader-Follower formation flight.

The wingtip vortex of the leading airplane imparts significant aerodynamic effects on the trailing airplane when they are flying co-altitude with opposing wingtips aligned and with a nose-to-tail separation on the order of four wingspans or less.[4] The two most observable vortex effects are rolling moment and drag force, $[\Delta C_l, \Delta C_D]$, which change quickly as a function of lateral and vertical spacing but gradually with nose-to-tail spacing.

A nonlinear vortex model for an F/A-18 airplane has been developed as part of the NASA Autonomous Formation Flight (AFF) project.[13] For this analysis, the model was simplified by assuming no vertical separation or bank angle difference between the two aircraft and that the lift coefficient of the leading airplane remains constant. Future expansion of this research will address these important effects. The drag output of the model is expressed in terms of percent change in induced drag. The percent change in total drag was estimated by assuming that induced drag makes up 50 percent of the total drag of the trailing airplane.[14] The predicted percent change in total drag force and incremental rolling moment coefficient are shown in figure 2 as a function of the lateral spacing between the aircraft given the preceding assumptions.

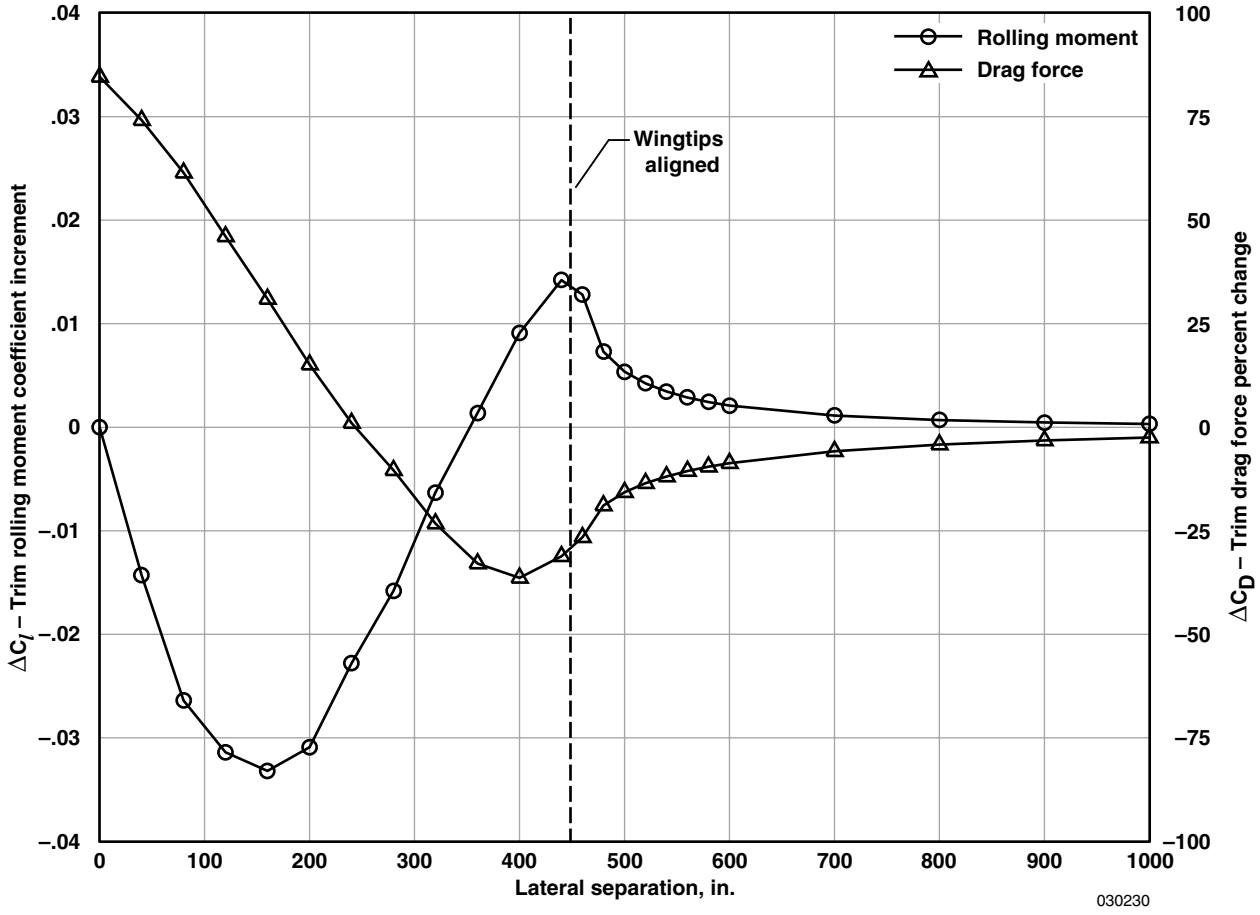

Figure 2. Vortex roll and drag effects.

FUZZY NAVIGATION ALGORITHM DESIGN

A fuzzy logic algorithm was explored as a means to capture the nonlinear, yet readily observable, relationship in figure 2 between combinations of vortex-induced aerodynamic effects and relative lateral position. Fuzzy logic is inherently nonlinear and allows the explicit definition of rules that address off-nominal conditions. Although not addressed in this report, fuzzy logic may also be transformed into an adaptive system, potentially providing a framework for addressing variables such as flight condition.

Figure 3 shows the processes involved in the fuzzy navigation. The algorithm first converts the crisp input estimates $\left[\Delta\hat{C}_l, \Delta\hat{C}_D\right]$ to fuzzy values $\left[\Delta\hat{C}_l^f, \Delta\hat{C}_D^f\right]$, then applies a set of inference rules to produce a fuzzy estimate of the relative lateral position $\hat{y}^f$, and finally computes the crisp estimate $\hat{y}$. The following three sections discuss each of these steps in further detail.

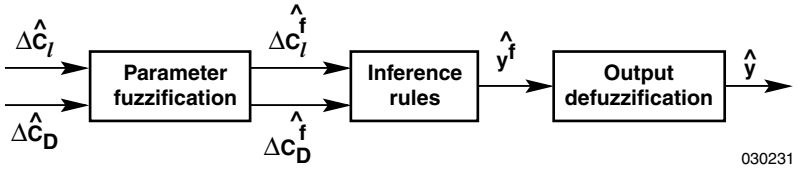

Figure 3. Fuzzy logic estimation algorithm.

Parameter Fuzzification

The lateral-axis fuzzy algorithm is a two-input, single-output system. Three fuzzy variables $\left[\Delta\hat{C}_l^f, \Delta\hat{C}_D^f, \hat{y}^f\right]$ are defined to correspond to the three observed crisp parameters $\left[\Delta\hat{C}_l, \Delta\hat{C}_D, \hat{y}\right]$ of the system. Parameter fuzzification is the process of mapping crisp input parameters to their associated fuzzy variables so that logical inference rules may be applied.

A fuzzy variable has a degree of membership between zero and one in each of a series of fuzzy sets defined across its universe of discourse. Fuzzy sets typically represent linguistic terms that an expert might use when applying decision rules for the system. A fuzzy membership function relates the value of a crisp parameter to a degree of membership in a particular fuzzy set of the corresponding fuzzy variable.

The universe of discourse for $\Delta\hat{C}_l$ is divided into 12 fuzzy sets ranging from negative extra large (NX) to positive extra large (PX). The universe of discourse for $\Delta\hat{C}_D$ is similarly divided into 10 fuzzy sets. Triangular input membership functions are chosen such that they cross at their midpoints, as shown in figure 4. The extreme endpoints of both the negative-most and positive-most membership functions are selected as negative and positive infinity, respectively. This approach constrains the sum total degree of membership of each fuzzy variable in all of its fuzzy sets to be exactly equal to one for any value of its associated crisp parameter within the universe of discourse.

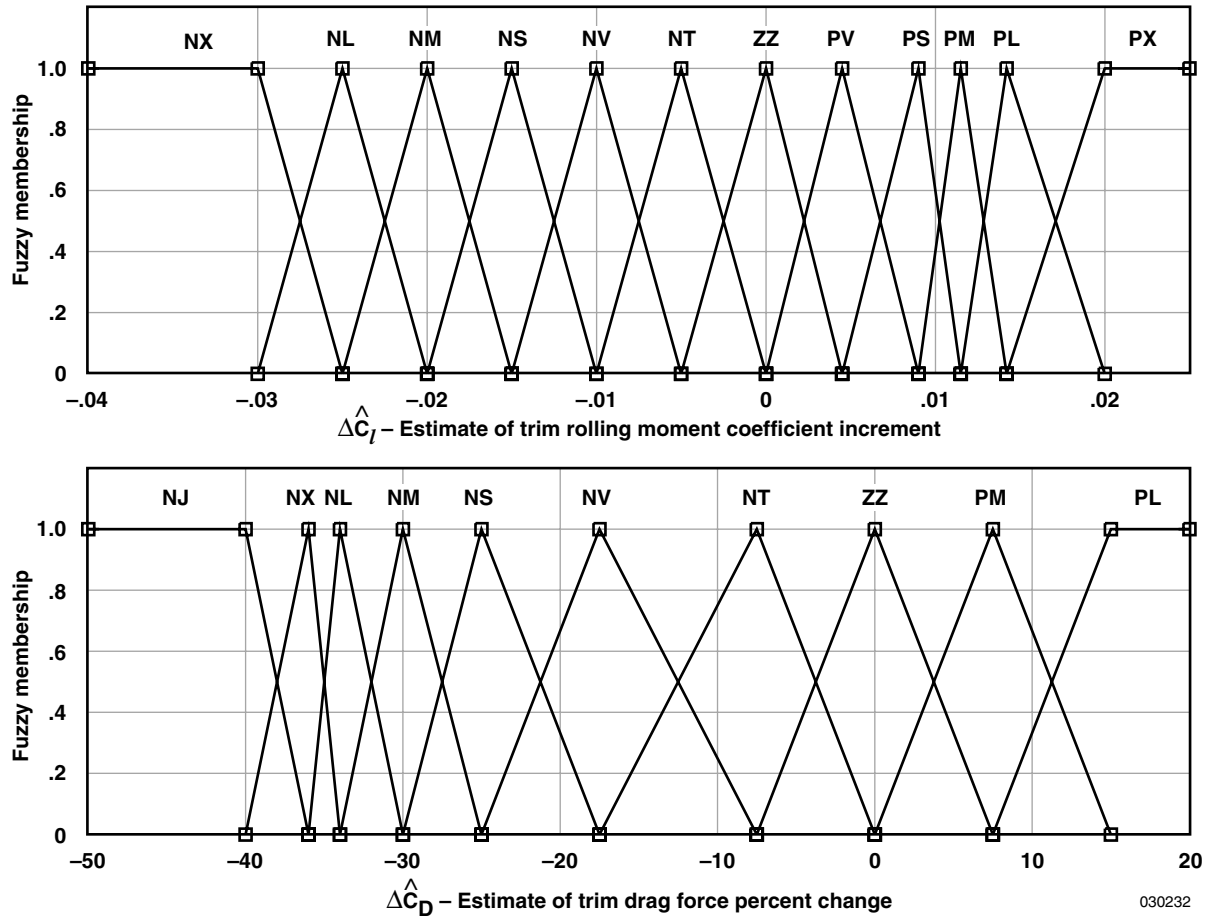

Figure 4. Input fuzzy membership functions.

The output of the fuzzy algorithm is an estimate of lateral relative position. Fourteen fuzzy sets are defined for the fuzzy output variable $\hat{y}^f$. The output membership functions, shown in figure 5 as they relate to the wingspan of the leading airplane, are defined as triangular functions with similar properties to the input membership functions described previously.

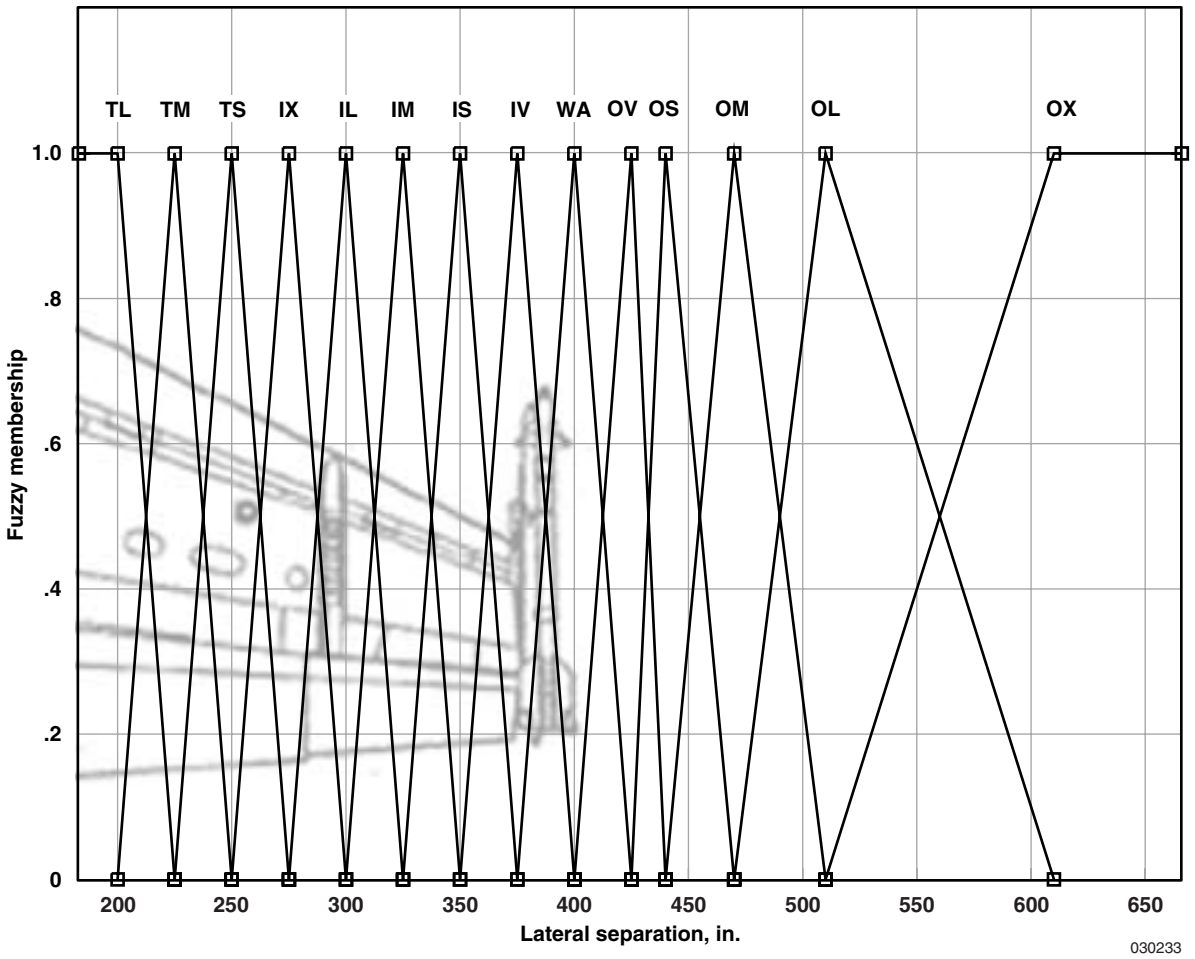

Figure 5. Output fuzzy membership functions.

The number of input and output fuzzy sets and the center point locations of their membership functions are selected based upon knowledge of the relationship between the two inputs and the output. Unique combinations of the two inputs that provide an accurate estimate of the lateral separation were identified using the F/A-18 aircraft vortex model.[13] Fuzzy set membership functions for each of the inputs were initially selected such that they spanned the range of vortex effects in a piecewise linear manner of relatively coarse resolution on the order of four to six sets. For the entire range of lateral position, the corresponding crisp rolling moment was determined and a graph of its degree of membership in all of its fuzzy sets was overlayed with similar information about drag force. Additional sets were added and existing membership function locations were adjusted in an attempt to align as closely as possible the lateral position at which both roll and drag achieved 100-percent membership. This common point was chosen as the desired centroid location of an output set membership function, and the two inputs sets were encoded into an inference rule.

Inference Rules

The inference rules of the fuzzy algorithm encapsulate knowledge of how combinations of vortex-induced aerodynamic effects correspond to lateral relative position. For a multiple-input, single-output fuzzy system, the maximum number of possible inference rules K is a function of the number of input variable fuzzy sets m_i defined for each of the i^{th} fuzzy input variables as:

$$K = \prod_{i=1}^{n} m_i \tag{1}$$

where n is the number of fuzzy input variables.

Inference rules for the two-input, single-output fuzzy algorithm assume the form of an if-then structure:

$$\textbf{if } \Delta\hat{C}_l^f \textbf{ is } A_1^{j_1} \textbf{ and } \Delta\hat{C}_D^f \textbf{ is } A_2^{j_2} \textbf{ then } \hat{y}^f = B_k \tag{2}$$

where $A_i^{j_i}(j_i = 1 \ldots m_i)$ are the fuzzy sets for the i^{th} input, $\hat{y}^f$ is the fuzzy output, and $B_k(k = 1 \ldots K)$ are the fuzzy output sets.[15] The rule is evaluated by determining the combined degree of truth of the antecedents ($A_i^{j_i}$) and assigning that degree of truth to the consequent (B_k).

The inference rules for a two-input, single-output system can be described as a matrix with K elements, where the m_1 rows represent fuzzy sets of the first fuzzy input variable and the m_2 columns represent fuzzy sets of the second. Each row-column pair defines the antecedents $A_1^{j_1}$ and $A_2^{j_2}$ of a potential fuzzy inference rule. The value of the corresponding matrix element is the consequent B_k, a fuzzy output set. In some instances, a fuzzy rule will encompass multiple fuzzy sets of a single antecedent. These sets are combined by adding their degrees of membership together.

Note that not all of the K possible rules are necessarily meaningful or useful. Inference rules for the fuzzy navigation algorithm are represented as a matrix in table 1. Of the possible $K = 120$ fuzzy inference rules, only 14 are nontrivial, corresponding to the 14 fuzzy output sets. Multiple fuzzy set antecedents are shown bounded by a dashed line.

Table 1. Fuzzy estimator interference rules.

$\Delta\hat{C}_l$ \ $\Delta\hat{C}_D$	PL	PM	ZZ	NT	NV	NS	NM	NL	NX	NJ
PX	—	—	—	—	—	—	—	—	—	—
PL	—	—	—	—	—	—	OS	—	—	—
PM	—	—	—	—	—	—	—	OV	—	—
PS	—	—	—	—	OM	—	—	—	WA	—
PV	—	—	—	OX	OL	—	—	IV	—	—
ZZ	—	—	—	OX	—	—	IS	—	—	—
NT	—	—	—	—	—	IM	—	—	—	—
NV	—	—	—	—	IL	—	—	—	—	—
NS	—	—	—	IX	—	—	—	—	—	—
NM	—	—	TS	—	—	—	—	—	—	—
NL	—	TM	—	—	—	—	—	—	—	—
NX	TL	—	—	—	—	—	—	—	—	—

Note: Dashed lines represent multiple fuzzy set antecedents.

In order to evaluate the inference rule (2), the individual degrees of truth of each antecedent are combined through the conjunctive **and** operator using any of a number of inference procedures. The correlation-minimum approach is applied here as:

$$\beta_k = \min\left(\alpha_1^{j_1}, \alpha_2^{j_2}\right) \tag{3}$$

where β_k is the resulting degree of membership, or truth, of the fuzzy output $\hat{y}^f$ in the fuzzy set B_k and $\alpha_i^{j_i}$ is the degree of membership of the i^{th} fuzzy input in the fuzzy set $A_i^{j_i}$.[15] The correlation-minimum approach is selected for its ability to eliminate ambiguities in each input by only returning nonzero degrees of membership if both antecedents are nonzero. When all of the inference rules are evaluated, the degree of membership of the fuzzy output variable in each of its fuzzy sets is known.

Output Defuzzification

In order to relate the lateral relative position fuzzy output variable $\hat{y}^f$ to its crisp counterpart $\hat{y}$, it must be defuzzified. As with fuzzy inference procedures, a number of different methods are available for output defuzzification. Due to its simplicity, the fuzzy centroid computation method was chosen as:

$$\hat{y} = \frac{\sum_{k=1}^{K} \beta_k \bar{b}_k}{\sum_{k=1}^{K} \beta_k} \tag{4}$$

where $\bar{b}_k$ is the centroid location of the k^{th} partially activated fuzzy output membership function.[15] Figure 6 shows a nonsymmetric triangular fuzzy output membership function reduced to a trapezoid according to its degree of activation. The centroid location is computed as:

$$\bar{b}_k = \frac{\left(b_{k-1} + b_{k+1}\right)\left(\beta_k^2 - 3 * \beta_k + 3\right) - b_k\left(2 * \beta_k^2 - 3 * \beta_k\right)}{6 - 3 * \beta_k} \tag{5}$$

where $[b_{k-1}, b_k, b_{k+1}]$ are the breakpoints of the membership function. When β is equal to one, $\bar{b}_k$ simplifies to the centroid location of the fully-activated triangular output membership function.

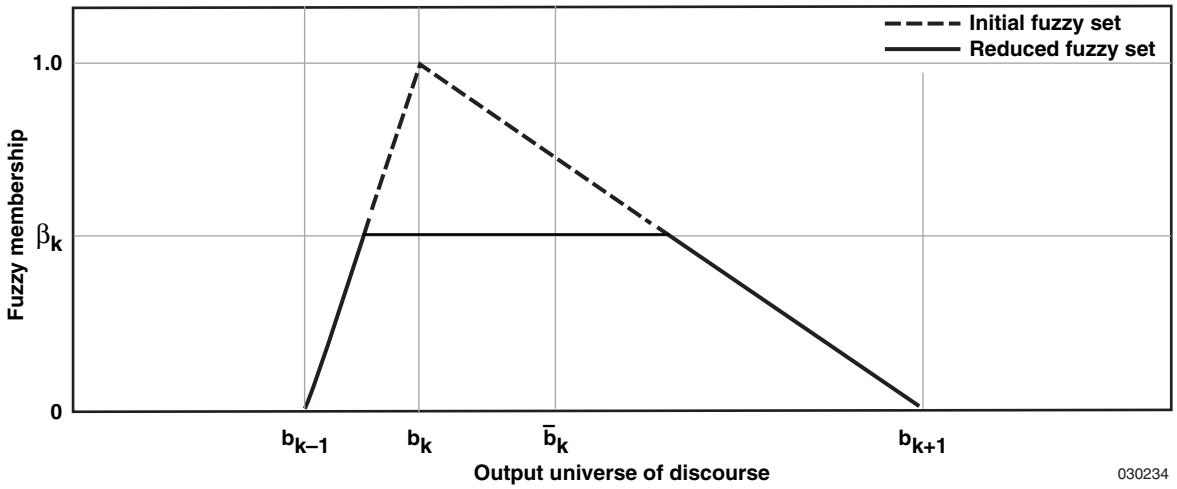

Figure 6. Reduced fuzzy output set.

FUZZY NAVIGATION ALGORITHM TUNING

The fuzzy algorithm was tuned off-line using vortex models to improve the quality of its estimations by adjusting the initial observation-based design. Parameter tuning is achieved by attempting to optimize the locations of the fuzzy membership functions. The tuning is a two-step iterative process by which the input membership functions are first adjusted while the output functions remain fixed; and then the output functions are adjusted while holding the new input functions fixed. The fuzzy inference rules are not modified.

Input Fuzzy Membership Function Tuning

Recall that triangular membership functions were chosen. The set of membership functions for the i^{th} fuzzy input are defined by their peak locations $a_i^{j_i}(j_i = 1 \ldots m_i)$ across the input universe of discourse. The fuzzy input membership functions are tuned using a simple dither search technique. The peak of each membership function is adjusted in both the negative and positive directions as follows:

$$\left.\begin{aligned} a_i^{j_i(-)} &= a_i^{j_i} - \sigma\left(a_i^{j_i} - a_i^{j_i-1}\right) \\ a_i^{j_i(+)} &= a_i^{j_i} + \sigma\left(a_i^{j_i+1} - a_i^{j_i}\right) \end{aligned}\right|_{j_i = 1 \ldots m_i} \tag{6}$$

where σ is the desired ratio of dither magnitude to the available room for tuning. The dither ratio parameter decreases the tuning step size as two peaks approach each other, preventing them from crossing each other. Figure 7 shows a sample universe of discourse containing three triangular fuzzy membership functions and their peaks.

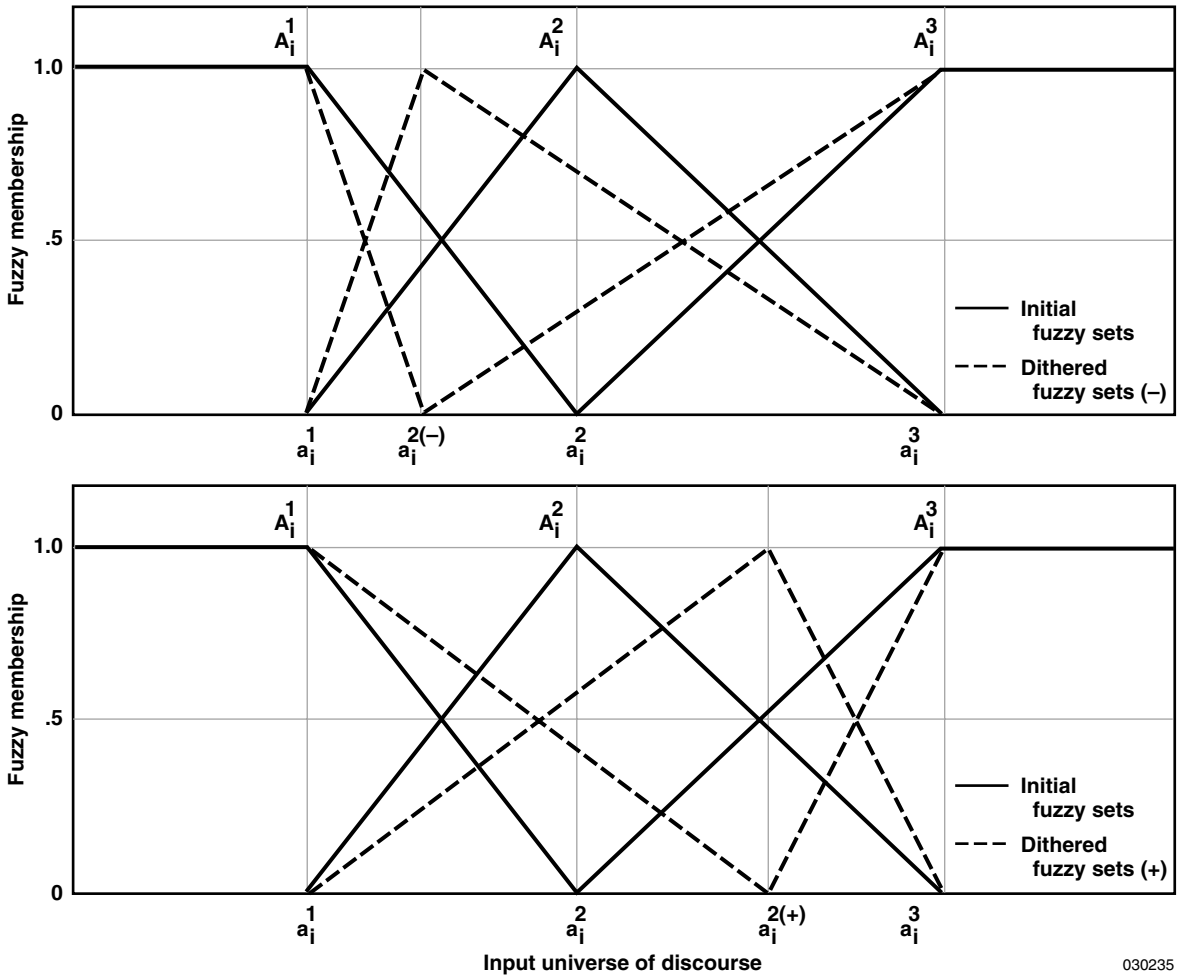

Figure 7. Input universe of discourse with three fuzzy membership functions.

A set of input-output training data is used to evaluate the resulting three potential peaks $\left[a_i^{j_i(-)}, a_i^{j_i}, a_i^{j_i(+)}\right]$ for each fuzzy membership function. The cost function J for each potential peak is calculated as:

$$J = \frac{\sum_{p=1}^{P} (y_p - \hat{y}_p)^2}{P} \tag{7}$$

where P is the number of training data points, y_p is the test data output, and $\hat{y}_p$ is the fuzzy estimate output. The potential membership function peak corresponding to the lowest cost function is retained.

Output Fuzzy Membership Function Tuning

Just as with the fuzzy input variables, the triangular output fuzzy set membership functions are defined by their peak locations $b_k (k = 1 \ldots K)$. Note that in this instance, K refers to the output fuzzy sets corresponding to the nontrivial inference rules rather than the larger group of potential rules defined in equation (1).

A gradient descent method is used to adjust the peak of each output fuzzy membership function based upon a set of input-output training data.[16] The partial derivative of the cost function J with respect to the output membership function centroid location $\bar{b}_k$ is calculated after substituting equations (4) and (5) into equation (7). The peak location adjustment is given by:

$$\Delta b_k = \eta \left(\frac{\sum_{p=1}^{P} (y_p - \hat{y}_p)}{P} \right) \left(\frac{\beta_k}{\sum_{k=1}^{K} \beta_k} \right) \left(\frac{2\beta_k^2 - 3\beta_k}{6 - 3 * \beta_k} \right) \tag{8}$$

where η is the tuning speed parameter. The peak location adjustments are constrained to be less than the distance to the nearest neighboring peak to prevent crossing. Also, the centers of gravity of the negative-most and positive-most membership functions are not adjusted in order to constrain the universe of discourse.

Design Results

The fuzzy lateral position navigation algorithm was tested by assuming a lateral position y for the trailing airplane within the region of vortex effects and computing the rolling moment and drag force change using the F/A-18 aircraft vortex model. The crisp values for ΔC_l and ΔC_D were input to the fuzzy algorithm, and the resulting crisp lateral separation estimate $\hat{y}$ was compared to the truth value y.

Since the peak drag reduction, and therefore the primary operating area, appears in the vicinity of 400 in., only lateral separations between 200 and 600 in. (in 10-in. increments) were evaluated.

The cost function from equation (7) and the estimate error:

$$\varepsilon = y - \hat{y} \tag{9}$$

are shown in figure 8 as functions of the true lateral separation. Results from both the initial and tuned fuzzy algorithms show that the maximum estimate error was reduced from approximately 36 in. to less than 14 in. Six tuning iterations were required to find the best solution with a dither ratio magnitude $\sigma = 0.1$ and tuning speed parameter $\eta = 3$. The tuned input fuzzy sets membership functions are shown in figure 9 along with the initial functions. The degree of tuning required was very small, generally only a few percent of the initial function width for a given set. The results are similar for the output fuzzy sets. The maximum and average tuning magnitudes for all three fuzzy variables are listed in table 2 as percentages of the initial width of each fuzzy set membership function.

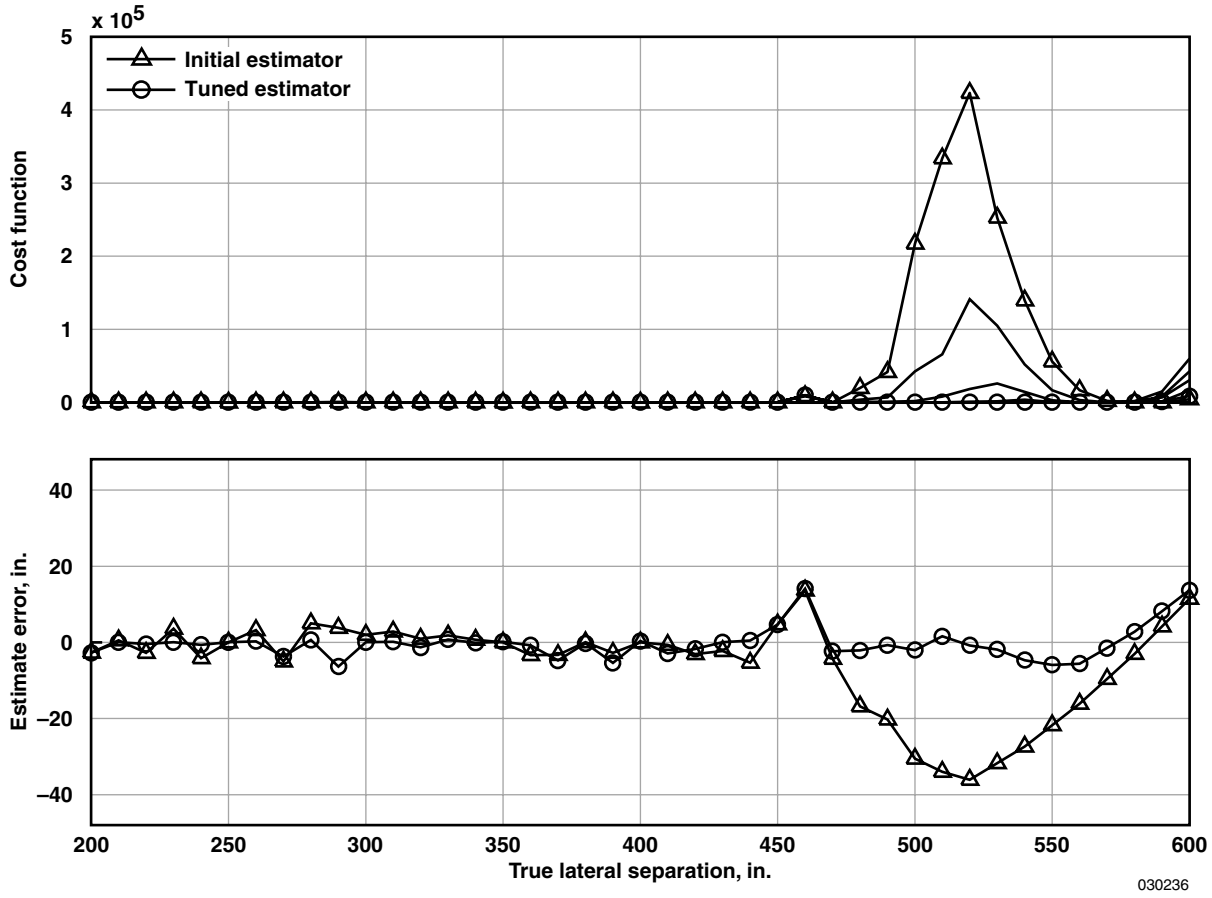

Figure 8. Lateral position estimate results.

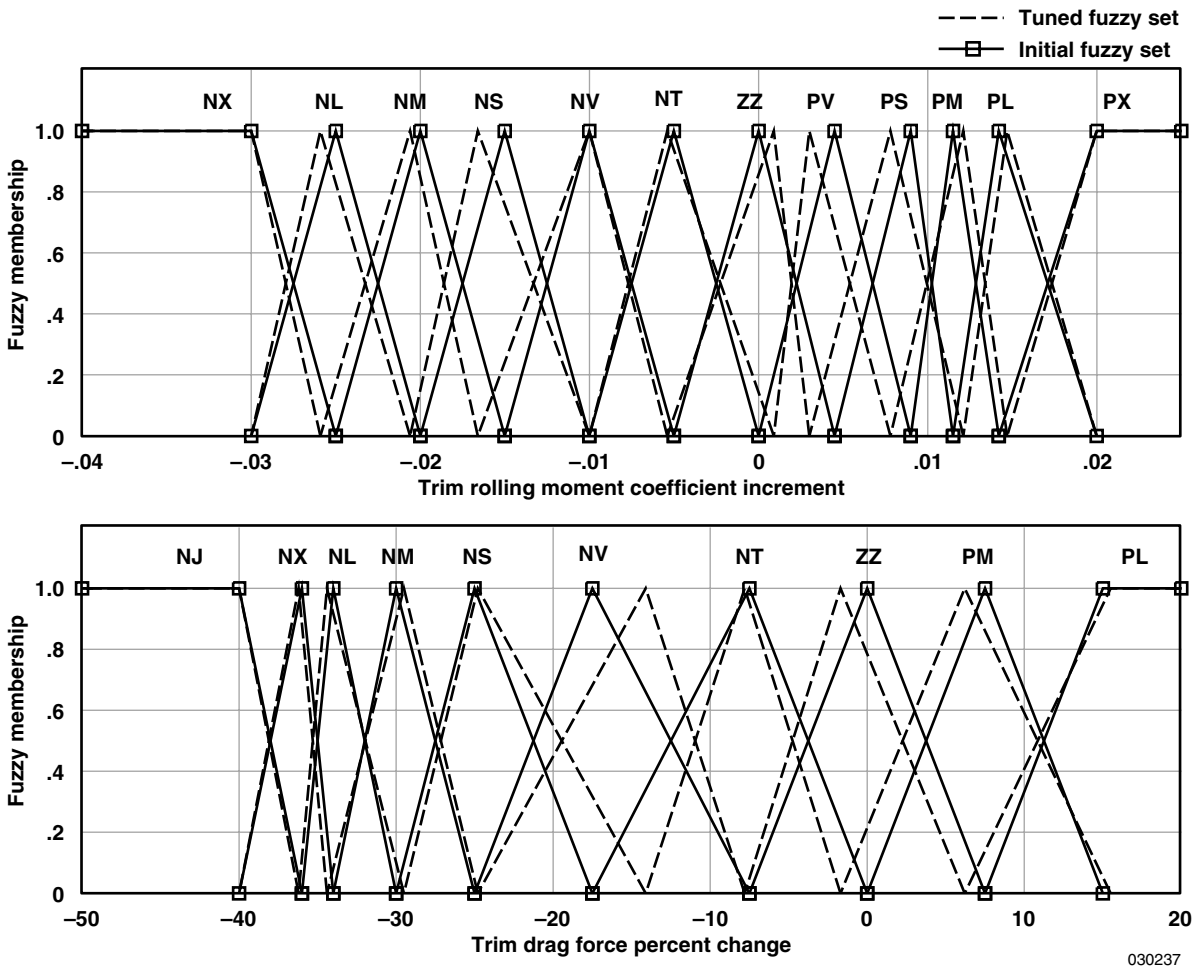

Figure 9. Tuned input fuzzy sets.

Table 2. Fuzzy estimator tuning magnitudes.

Fuzzy sets	Maximum tuning magnitude, percent	Average tuning magnitude, percent
$\Delta \hat{C}_l^f$	17	8
$\Delta \hat{C}_D^f$	19	6
$\hat{y}^f$	4	1

EFFECTS OF INPUT BIASES

Although the design presented in the previous section provides reasonably accurate estimates for perfect inputs, the algorithm must be augmented with the rules that describe how to handle inputs that fall outside of the currently defined bounds of the system. Recall that the current fuzzy system is only defined for 14 of the possible 120 inference rules. Uncertain inputs tend to result in combinations of fuzzy input variables for which no rule has been defined. Although in practice it might be better to retain the last known good output in these instances, the author has chosen instead to define the output of the algorithm as zero lateral separation in order to make these instances more identifiable when observing the simulation results.

The response of the fuzzy navigation algorithm to input uncertainties was improved by populating the inference rules that are considered trivial for a nominal system. The system inputs were deliberately biased and auxillary rules were developed by observing the relationships between the corresponding fuzzy input variables and the estimated output. The new auxiliary rules were evaluated in the same manner as before, and their outputs were summed with the appropriate outputs of the primary rules. Table 3 shows an expanded set of fuzzy inference rules for the system designed to improve its response to combined positive and negative biases on the roll and drag inputs. The primary rules, the same as in table 1, are shown in black and the auxiliary rules are written in gray.

Table 3. Expanded fuzzy estimator inference rules.

$\Delta\hat{C}_I$ \ $\Delta\hat{C}_D$	PL	PM	ZZ	NT	NV	NS	NM	NL	NX	NJ
PX	—	—	—	—	—	OS	—	—	—	—
PL	—	—	—	—	—	—	OS	—	—	—
PM	—	—	—	—	OM	—	—	OV	—	—
PS	—	—	—	OX	OM	—	IV	—	WA	—
PV	—	—	—	OX	OL	—	—	IV	—	WA
ZZ	—	—	—	OX	—	IM	IS	—	—	IV
NT	—	—	—	—	IM	IM	—	IS	IS	—
NV	—	—	IX	IX	IL	—	IM	—	—	—
NS	—	TS	TS	IX	—	IL	—	—	—	—
NM	—	TS	TS	—	IX	—	—	—	—	—
NL	TM	TM	—	TS	—	—	—	—	—	—
NX	TL	TM	TM	—	—	—	—	—	—	—

Note: Dashed lines represent multiple fuzzy set antecedents.

The augmented tuned fuzzy algorithm was analyzed to determine its sensitivity to measurement errors. Four scenarios were analyzed: all combinations of simultaneous positive and negative biases on both inputs. In each scenario, the magnitude of the bias was chosen as ten percent of the total expected range of each input. The same input vector was used as before for lateral separation values ranging from 200 to 600 in. (in 10-in. increments). The biases were applied to the calculated crisp values of ΔC_l and ΔC_D prior to fuzzification.

Figure 10 shows estimate errors for each scenario. Even with fairly large input biases, the estimates maintain an accuracy of approximately 50 in. for most lateral separations less than 450 in., corresponding to wing overlap. The accuracy grows progressively worse as the trailing airplane moves further outboard. In this region, the biased inputs tend to cause larger shifts in the estimated output as a result of the shallower slopes of both vortex effects. Because the area of significant drag reduction occurs inboard of approximately 500 in. of lateral separation, closed-loop system performance may be adequate despite these types of input uncertainties.

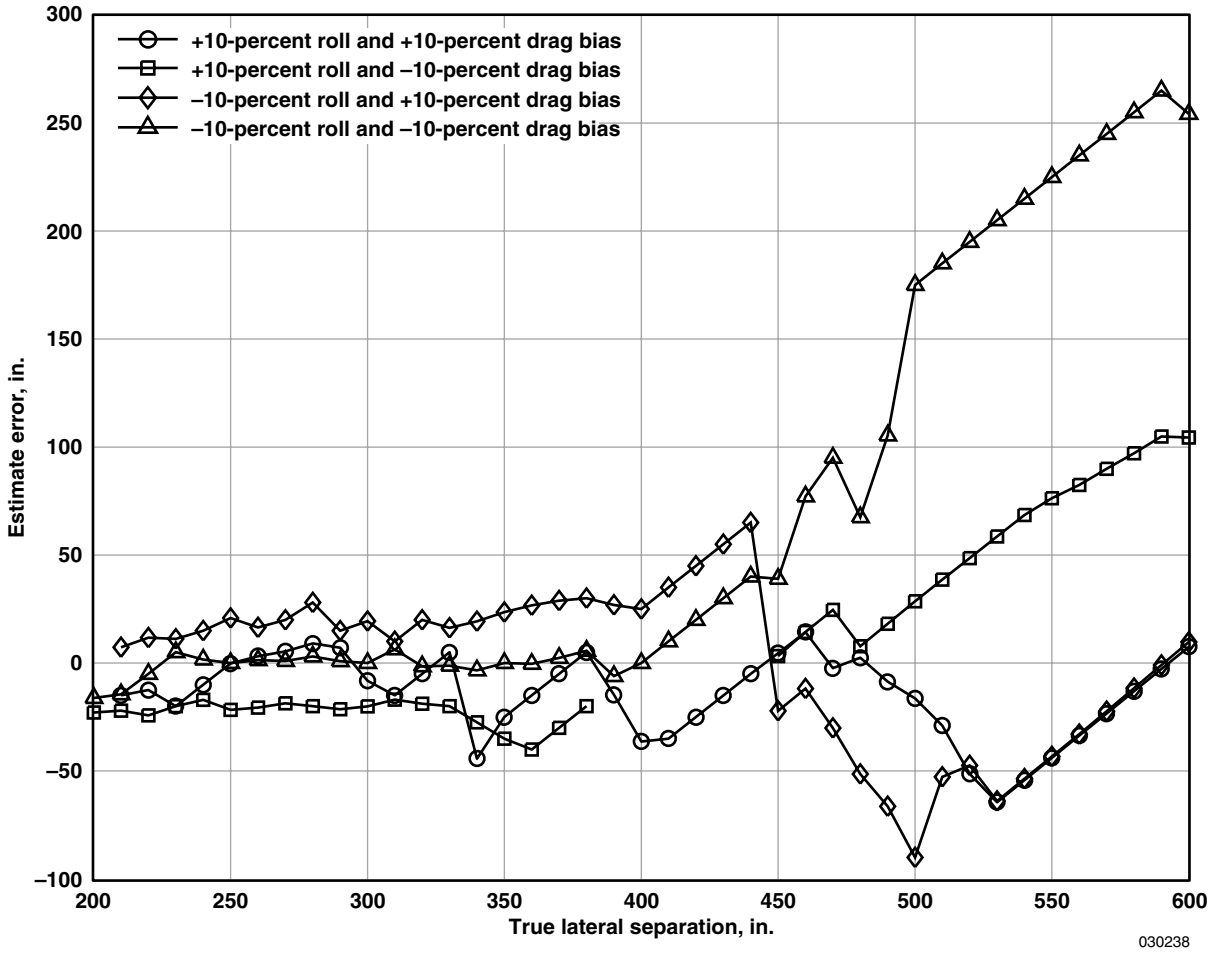

Figure 10. Effects of input biases.

CLOSED-LOOP EVALUATION

To evaluate the usefulness of the fuzzy navigation algorithm in a closed-loop system, the algorithm was integrated into a simulation of two F/A-18 aircraft. Each airplane model consisted of a linear bare airframe model with an inner-loop control system and outer-loop autopilot control for altitude and velocity. For the leading airplane, lateral control was accomplished by a heading-hold autopilot. The trailing airplane was outfitted with a linear lateral formation separation controller designed to track movements of the leading airplane while rejecting vortex disturbances.[7,8] Figure 11 shows the lateral formation control system augmented by the fuzzy navigation algorithm. To simplify modeling, the control system and fuzzy algorithm operate at 80 Hz, the highest rate of the F/A-18 aircraft inner-loop controller. In practice, outer-loop control at 20 Hz is generally adequate. The vortex-induced drag and side force as well as pitching, rolling, and yawing moment effects were modeled for the trailing airplane. Nose-to-tail separation effects were not modeled, and pilot inputs required to control nose-to-tail separation were not considered. Finally, each airplane was subjected to different lateral and vertical atmospheric turbulence in order to excite relative motion between them.

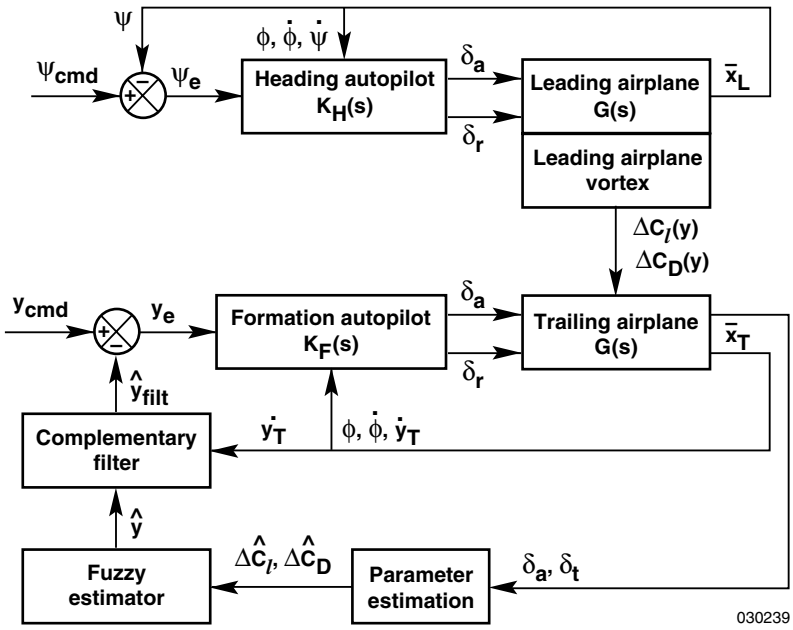

Figure 11. Lateral formation control with vortex-aided navigation.

Input Parameter Estimation

Until now, this report has assumed an on-line parameter estimation capability exists that can accurately provide real-time estimates of ΔC_l and ΔC_D. In practice, the rolling moment may be derived from the steady-state trim value of the lateral position controller, whose output is a command to the roll effecting actuators. Or, if available, the actuator positions of the roll effectors may be used instead. An estimate of the drag force change can be obtained by a comparison of the actual and expected throttle position or fuel flow for the given flight condition.

To evaluate the fuzzy navigation algorithm in a closed-loop sense, a simple linear parameter estimation approach was implemented in the simulation. Rolling moment was related through a scale factor to the roll stick command output of the lateral position controller onboard the trailing airplane. Similarly, drag force change was related to the throttle command output of the velocity-hold autopilot onboard the trailing airplane through a scale factor. The resulting estimates of the vortex-induced aerodynamic effects were used as inputs to the fuzzy algorithm.

Closed-Loop Integration

The lateral formation controller must simultaneously maintain the commanded spacing within the formation and reject the rolling moment disturbances of the vortex. Vortex disturbance rejection generally requires a higher bandwidth than control of formation spacing. The parameter estimation approach discussed previously produces its rolling moment estimates based upon both the low frequency trim outputs of the controller and the higher-frequency disturbance rejection commands. The low-frequency portion of the lateral position feedback from the fuzzy navigation algorithm is relied upon for formation guidance. Disturbance rejection can be achieved by feeding back the high-frequency content of the lateral position of the local airplane. Therefore, a complementary filter, as shown in figure 12, was designed to combine the output of the fuzzy lateral position estimate with the integrated local lateral velocity. A frequency breakpoint of one radian per second was selected.

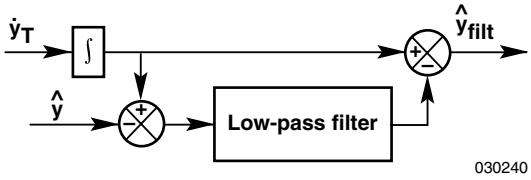

Figure 12. Complementary filter.

Closed-Loop Performance

A ten-minute simulation was performed in which both aircraft were initialized in formation at 480 in. of lateral separation, or just outboard of a wingtips aligned configuration. This position was chosen to avoid lateral formation autopilot stability problems nearer to the location of peak drag reduction, which are unrelated to the research presented in this report. The chosen formation spacing is also within the region in which the fuzzy navigation algorithm exhibits degraded accuracy due to input biases, allowing for a reasonably stringent test of the overall system performance.

Both aircraft were subjected to different lateral and vertical turbulence effects. Figure 13 shows the lateral position of both aircraft if the fuzzy estimate feedback is turned off and no intership communication is allowed. The leading airplane moves laterally by more than 1,000 in. while attempting to maintain a constant heading amid the turbulence. As expected, the trailing airplane fails to maintain the formation and instead continues to follow a straight line. The initial closing movement of the leading airplane causes the trailing airplane to encounter the extreme inboard portion of the vortex—a condition outside of the design envelope of the lateral formation autopilot and a region in which the autopilot is unstable. The trailing airplane rapidly exits the vortex and recovers, but fails to rejoin the leading airplane, ultimately ending up more than 1,500 in. out of position.

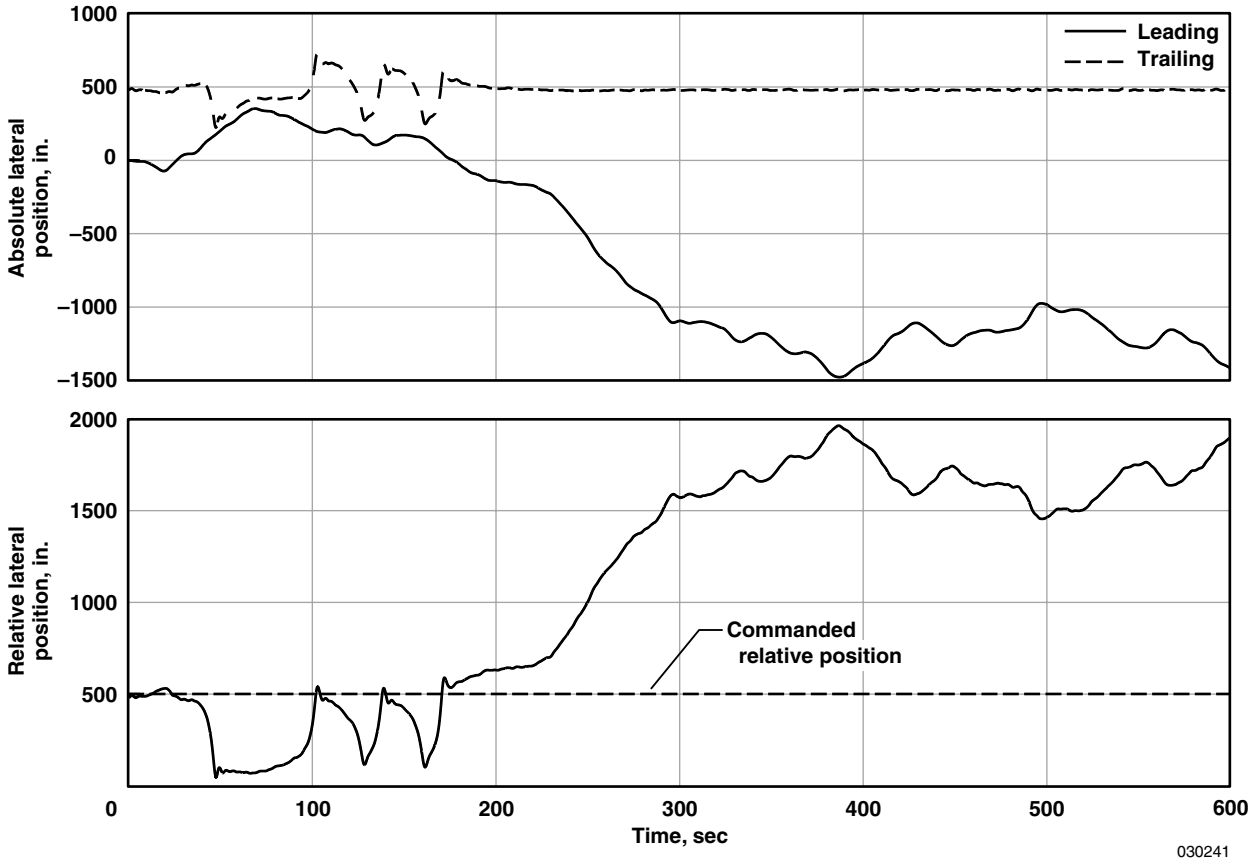

Figure 13. Formation tracking without fuzzy estimates or intership communication.

This test is then repeated with the fuzzy navigation algorithm activated. Figure 14 shows that for the same disturbances and leading airplane motion, the trailing airplane is able to maintain the formation. The lateral position errors are in the range of ±20 in. during most of the test. During the initial closing motion, the fuzzy estimate is fast enough even with the complementary filter to avoid the unstable region of the controller.

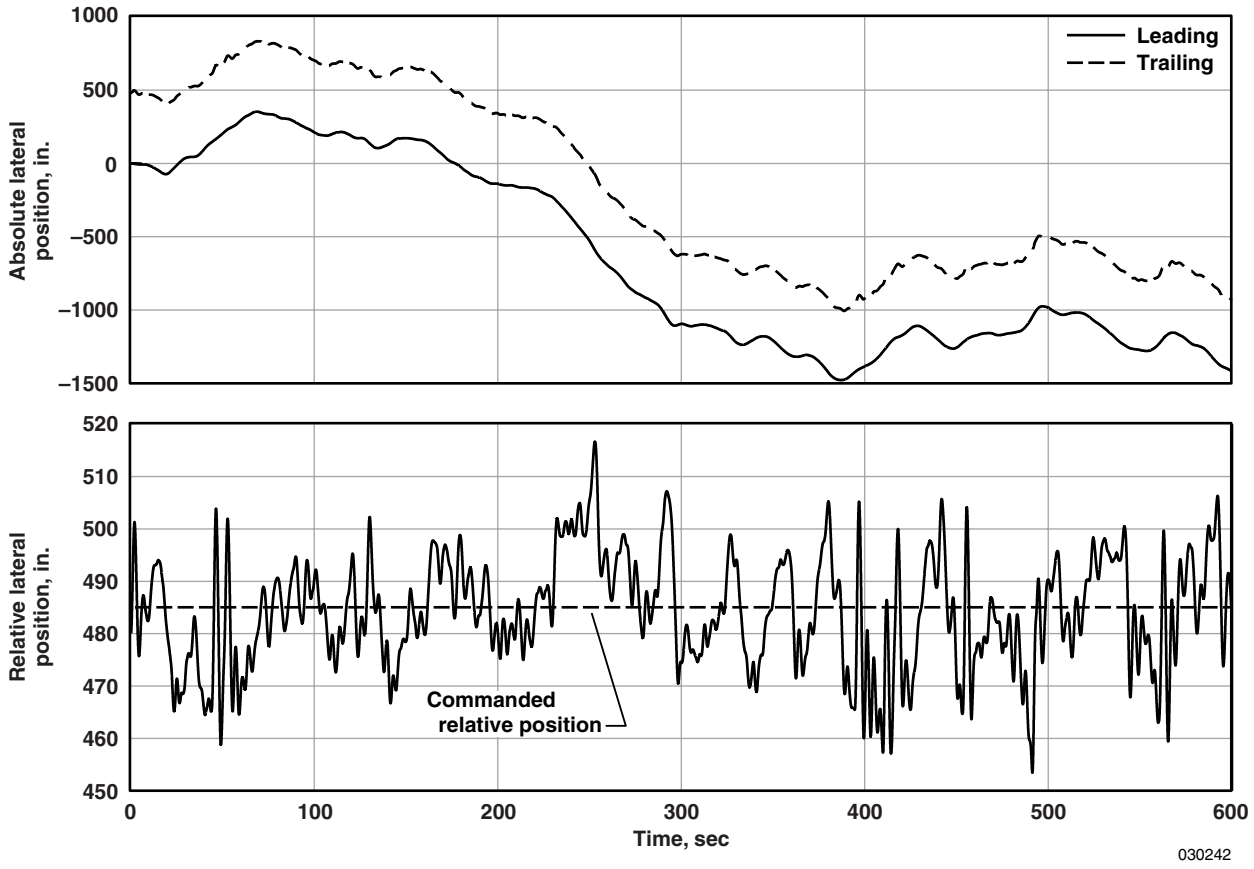

Figure 14. Tracking errors with fuzzy estimates.

Figure 15 shows the real and estimated vortex-induced rolling moment and the rolling moment parameter estimation error during the simulation discussed in the previous paragraph. Figure 16 similarly shows the real and estimated drag force and the associated parameter estimation error. The dashed lines represent ±10 percent of the total expected range of the input for comparison to the results of the previous section discussing input biases. As expected, the rolling moment is easier to characterize using these methods because of the responsiveness of the F/A-18 aircraft in the roll axis. Conversely, the sluggishness of the engine models in response to throttle commands results in less accurate drag force estimates. However, both estimate errors are generally less than the 10-percent magnitude evaluated previously and are accurate enough for use by the fuzzy navigation algorithm. Note that the drag force change is generally in the vicinity of a 17-percent reduction.

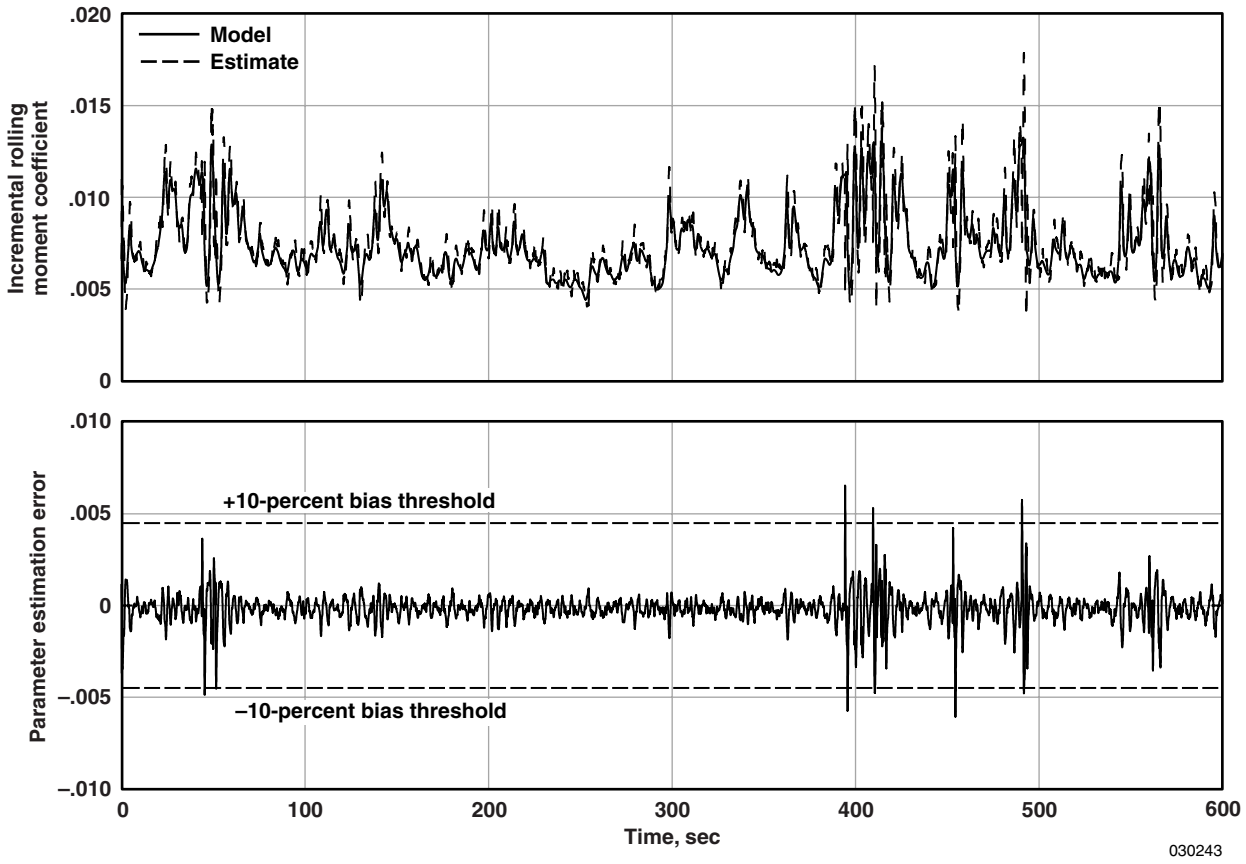

Figure 15. Roll parameter estimation results.

The fuzzy lateral position estimate is plotted against the true lateral position in figure 17, along with the estimate error. Occasionally, the combination of fuzzified aerodynamic effects fall outside of the defined fuzzy inference rules, and the algorithm exhibits large spikes in its lateral position estimates. When the algorithm is able to compute a valid solution, the error is generally less than 20 in., occasionally reaching as much as 40 in. An interesting aspect of the fuzzy estimate is the occurrence of what appears to be a limiting effect on the estimate as the relative lateral position drops below approximately 470 in. This apparent limiting is actually caused by a peak in estimate error in the same vicinity, as seen previously in figure 8. As the relative lateral position drops below 470 in., the error magnitude grows at approximately the same rate and in the opposite direction, causing the position estimate to appear saturated. The effect is relatively minor and does not significantly affect the system performance.

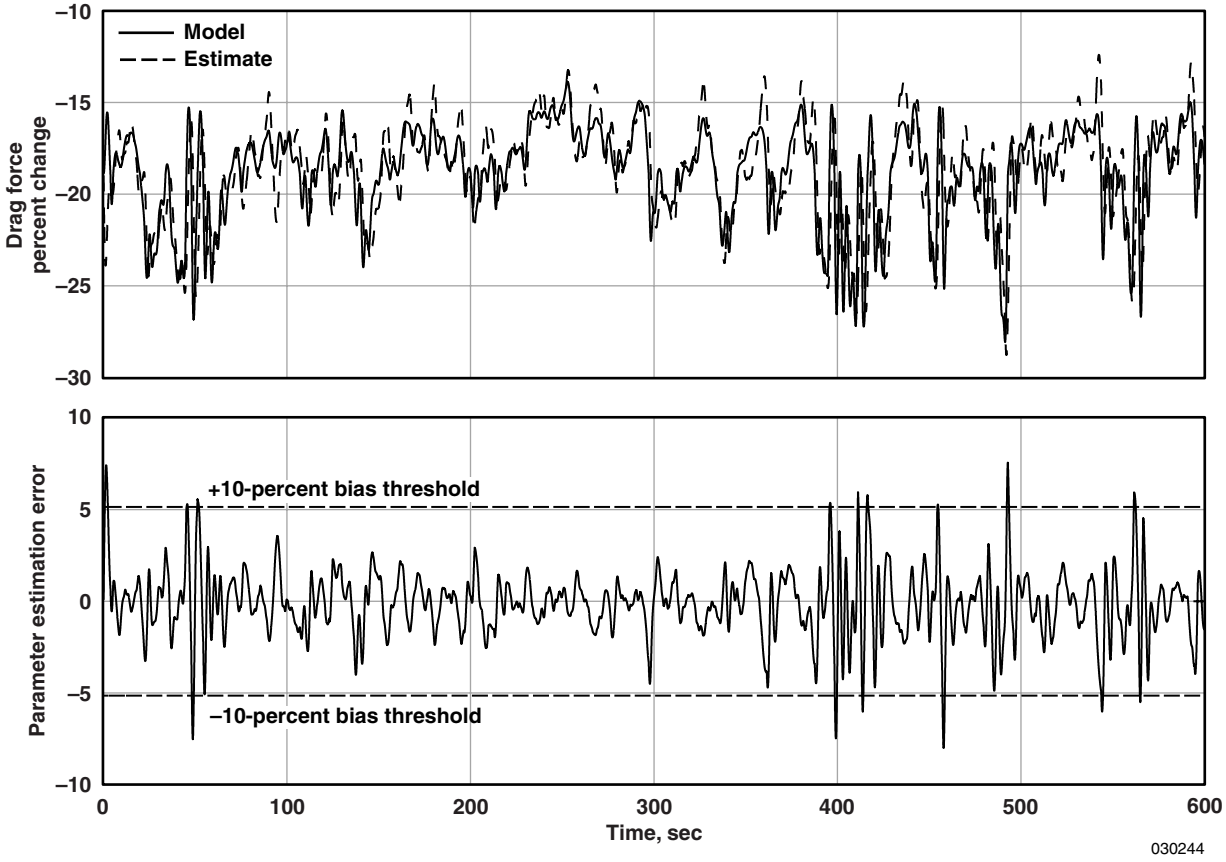

Figure 16. Drag parameter estimation results.

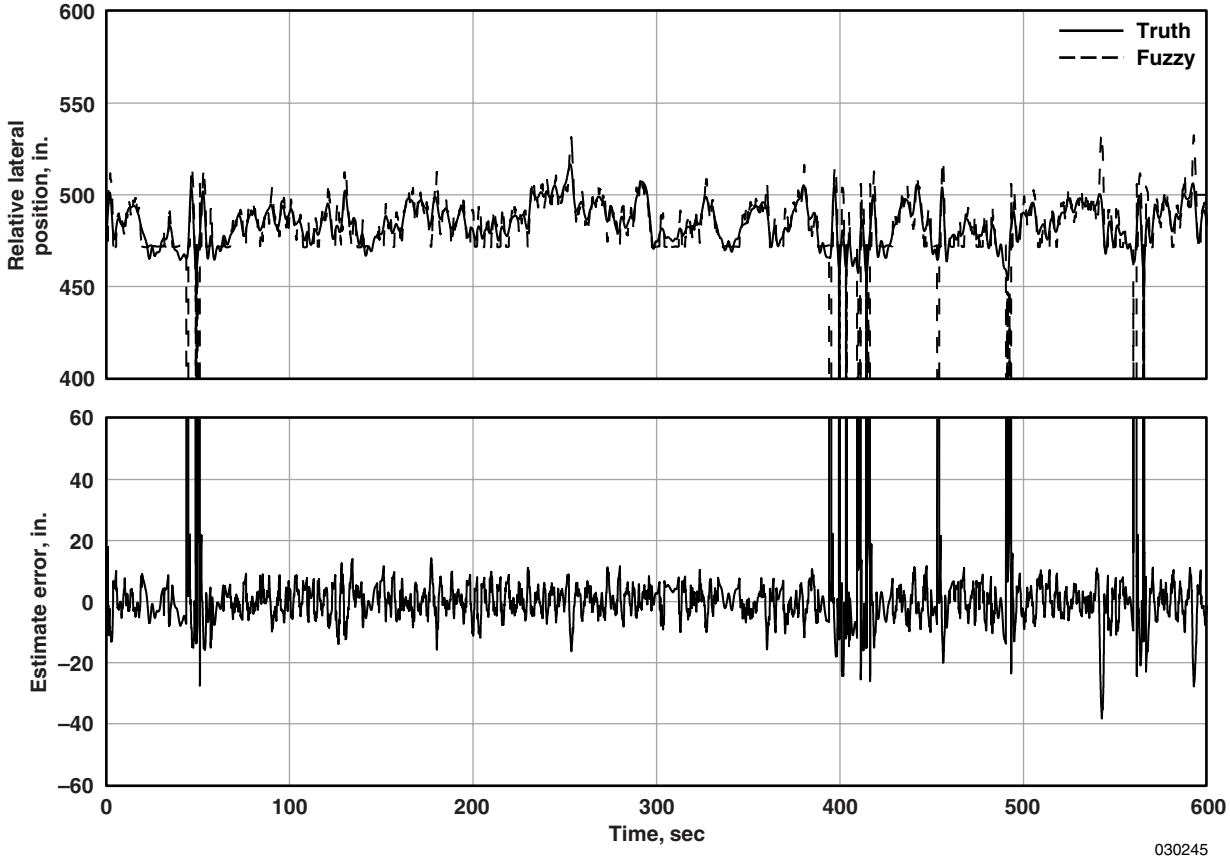

Figure 17. Fuzzy estimation algorithm results.

Figure 18 shows the spikes in the fuzzy output are sufficiently reduced in the final feedback by the complementary filter to produce good closed-loop results. As mentioned earlier, a value of zero was assigned to the output of the fuzzy algorithm in order to easily identify these occurrences when no solution was found. An approach such as holding the last known good value would further reduce the effects of out-of-bounds input data.

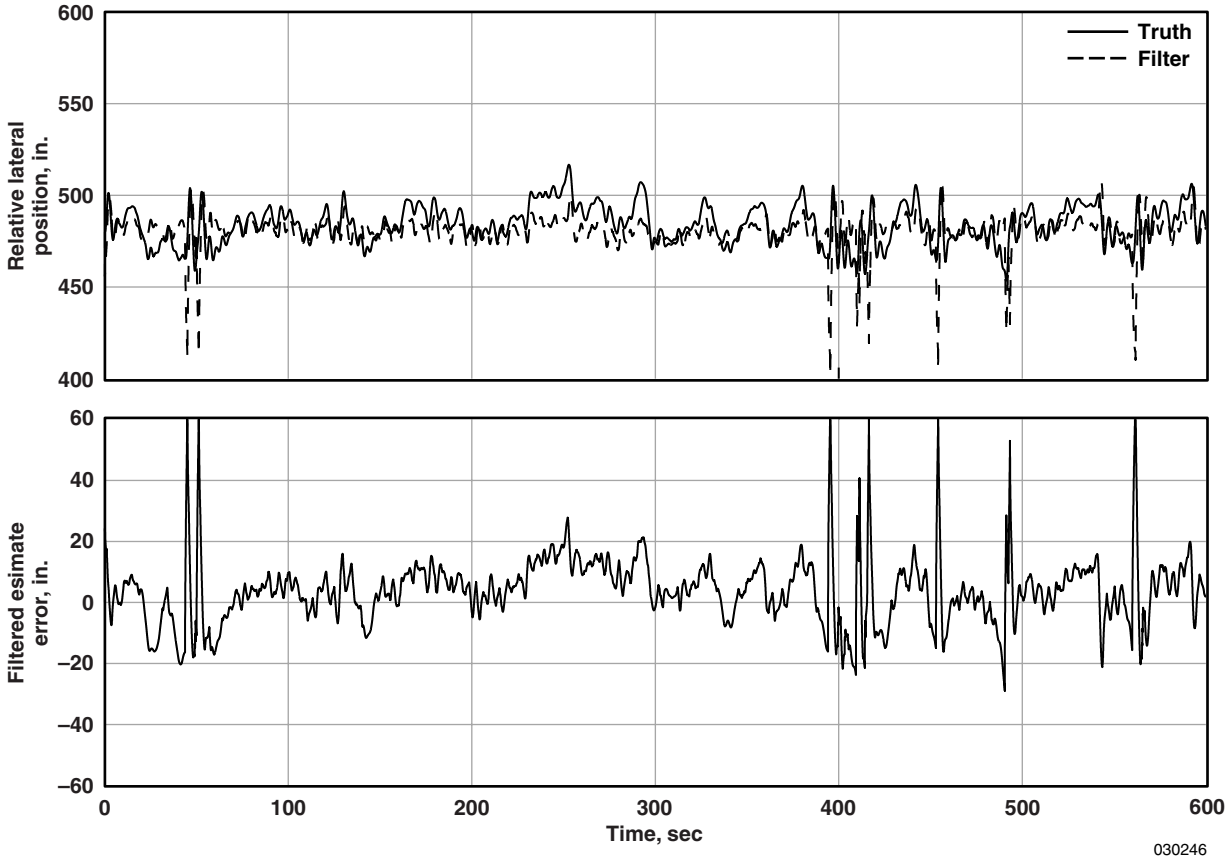

Figure 18. Filtered estimation results.

SUMMARY

The relationship between vortex-induced aerodynamic effects on a trailing F/A-18 airplane in close formation flight and the relative lateral position of a leading F/A-18 airplane was identified and encapsulated into a fuzzy logic-based navigation algorithm. The algorithm provided results accurate to within ±40 in. using an initial design based upon observed relationships. The fuzzy system was tuned over a set of training input and output data. The resulting estimate errors were reduced by nearly two-thirds to within ±14 in. The fuzzy algorithm was then augmented with additional inference rules to improve its response to input data uncertainty.

The fuzzy navigation algorithm was integrated with a lateral formation controller in a two-aircraft simulation that included a model of the vortex-induced force and moment effects on the trailing airplane. A simple parameter estimation scheme provided rolling moment and drag force estimates to the fuzzy system. Results show that without intership communication or predefined trajectories and in the presence of input uncertainties, the fuzzy algorithm generally provides estimates accurate to within ±20 in. The trailing airplane was able to maintain a significant level of drag reduction while tracking the motion of the leading airplane caused by turbulence effects.

This research shows that formation flight drag reduction without logistically burdensome intership communication or predefined trajectories may be possible, leading to a more likely acceptance of this technology by the commercial sector. This research may be extended towards a two-dimensional navigation solution by incorporating knowledge of how vortex effects change as a function of both lateral and vertical position. Means for implementing this type of vortex-based formation navigation solution other than fuzzy logic, such as Kalman filtering, are also under investigation.

REFERENCES

1. Beukenberg, Markus and Dietrich Hummel, "Aerodynamics, Performance and Control of Airplanes in Formation Flight," *ICAS Proceedings 1990: 17th Congress of the International Council of the Aeronautical Sciences*, Sept. 1990, pp. 1777–1794.

2. Hummel, Dietrich, "Formation Flight as an Energy-Saving Mechanism," *Israel Journal of Zoology*, Vol. 41, 1995, pp. 261–278.

3. Vachon, M. Jake, Ronald J. Ray, Kevin R. Walsh, and Kimberly Ennix, "F/A-18 Aircraft Performance Benefits Measured During the Autonomous Formation Flight Project," AIAA 2002-4491, Flight Mechanics Conference and Exhibit, Monterey, CA, Aug. 2002.

4. Hansen, Jennifer L. and Brent R. Cobleigh, "Induced Moment Effects of Formation Flight Using Two F/A-18 Aircraft," AIAA 2002-4489, Flight Mechanics Conference and Exhibit, Monterey, CA, Aug. 2002.

5. Wolfe, J. D., D. F. Chichka, and J. L. Speyer, "Decentralized Controllers for Unmanned Aerial Vehicle Formation Flight," AIAA 96-3833, July 1996.

6. Pachter, Meir, John J. D'Azzo, and Andrew W. Proud, "Tight Formation Flight Control," AIAA Journal of Guidance, Control and Dynamics, Vol. 24, No. 2, March–April 2001.

7. Lavretsky, Eugene, "F/A-18 Autonomous Formation Flight Control System Design," AIAA 2002-4757, AIAA Guidance, Navigation, and Control Conference and Exhibit, Monterey, CA, Aug. 2002.

8. Misovec, Kathleen, "Applied Adaptive Techniques for F/A-18 Formation Flight," AIAA 2002-4550, AIAA Guidance, Navigation, and Control Conference and Exhibit, Monterey, CA, Aug. 2002.

9. Singh, Sahjendra N., Rong Zhang, Phil Chandler, and Siva Banda, "Decentralized Adaptive Close Formation Control of UAV's," AIAA 2001-0106, 39th AIAA Aerospace Sciences Meeting & Exhibit, Reno, NV, Jan. 2001.

10. Bever, Glenn, Peter Urschel, and Curtis E. Hanson, *Comparison of Relative Navigation Solutions Applied Between Two Aircraft*, NASA/TM-2002-210728, June 2002.

11. Chichka, D. F., C. G. Park, and J. L. Speyer, "Peak-Seeking Control with Application to Formation Flight," CDC99-REG0600, 1999.

12. Hanson, Curtis E., Jack Ryan, Michael J. Allen, and Steven R. Jacobson, "An Overview of Flight Test Results for a Formation Flight Autopilot," AIAA 2002-4755, AIAA Guidance, Navigation, and Control Conference and Exhibit, Monterey, CA, Aug. 2002.

13. Dunn, Ken, *Calculated Aerodynamic Force and Moment Increments Induced on the Trailing Aircraft in a Two-Aircraft F-18 Formation*, Boeing North American, Inc., Long Beach, CA, 1999. (Distribution restricted to AFF Program participants.)

14. Ray, Ronald J., Brent R. Cobleigh, M. Jake Vachon, and Clinton St. John, "Flight Test Techniques Used to Evaluate Performance Benefits During Formation Flight," AIAA 2002-4492, AIAA Guidance, Navigation, and Control Conference and Exhibit, Monterey, CA, Aug. 2002.

15. Kosko, Bart, *Neural Networks and Fuzzy Systems*, Prentice-Hall, Inc., Englewood Cliffs, NJ, 1992.

16. Glorennec, Pierre Yves, "Learning Algorithms for Neuro-Fuzzy Networks," *Fuzzy Control Systems*, CRC Press, Inc., Boca Raton, FL, 1994.

REPORT DOCUMENTATION PAGE

Form Approved
OMB No. 0704-0188

1. AGENCY USE ONLY (Leave blank)	2. REPORT DATE	3. REPORT TYPE AND DATES COVERED
	September 2003	Technical Memorandum

4. TITLE AND SUBTITLE

A Fuzzy Technique for Performing Lateral-Axis Formation Flight Navigation Using Wingtip Vortices

5. FUNDING NUMBERS

710-35-14-SE-45-00-AAR

6. AUTHOR(S)

Curtis E. Hanson

7. PERFORMING ORGANIZATION NAME(S) AND ADDRESS(ES)

NASA Dryden Flight Research Center
P.O. Box 273
Edwards, California 93523-0273

8. PERFORMING ORGANIZATION REPORT NUMBER

H-2523

9. SPONSORING/MONITORING AGENCY NAME(S) AND ADDRESS(ES)

National Aeronautics and Space Administration
Washington, DC 20546-0001

10. SPONSORING/MONITORING AGENCY REPORT NUMBER

NASA/TM-2003-212033

11. SUPPLEMENTARY NOTES

12a. DISTRIBUTION/AVAILABILITY STATEMENT

Unclassified—Unlimited
Subject Category 08

This report is available at http://www.dfrc.nasa.gov/DTRS/

12b. DISTRIBUTION CODE

13. ABSTRACT (Maximum 200 words)

Close formation flight involving aerodynamic coupling through wingtip vortices shows significant promise to improve the efficiency of cooperative aircraft operations. Impediments to the application of this technology include intership communication required to establish precise relative positioning. This report proposes a method for estimating the lateral relative position between two aircraft in close formation flight through real-time estimates of the aerodynamic effects imparted by the leading airplane on the trailing airplane. A fuzzy algorithm is developed to map combinations of vortex-induced drag and roll effects to relative lateral spacing. The algorithm is refined using self-tuning techniques to provide lateral relative position estimates accurate to 14 in., well within the requirement to maintain significant levels of drag reduction. The fuzzy navigation algorithm is integrated with a leader-follower formation flight autopilot in a two-ship F/A-18 simulation with no intership communication modeled. It is shown that in the absence of measurements from the leading airplane the algorithm provides sufficient estimation of lateral formation spacing for the autopilot to maintain stable formation flight within the vortex. Formation autopilot trim commands are used to estimate vortex effects for the algorithm. The fuzzy algorithm is shown to operate satisfactorily with anticipated levels of input uncertainties.

14. SUBJECT TERMS

Automatic pilot, Drag reduction, Formation flying, Fuzzy system, Wingtip vortex

15. NUMBER OF PAGES

33

16. PRICE CODE

17. SECURITY CLASSIFICATION OF REPORT	18. SECURITY CLASSIFICATION OF THIS PAGE	19. SECURITY CLASSIFICATION OF ABSTRACT	20. LIMITATION OF ABSTRACT
Unclassified	Unclassified	Unclassified	Unlimited